AMERICAN SOCIETY FOR MICROBIOLOGY | Infection and Immunity®

HOST RESPONSE AND INFLAMMATION

A Murine Model for Enhancement of *Streptococcus pneumoniae* Pathogenicity upon Viral Infection and Advanced Age

Basma H. Joma,[a,b] Nalat Siwapornchai,[a] Vijay K. Vanguri,[c] Anishma Shrestha,[a] Sara E. Roggensack,[a,d] Bruce A. Davidson,[e] Albert K. Tai,[f] Anders P. Hakansson,[g] Simin N. Meydani,[h] John M. Leong,[a,i] Elsa N. Bou Ghanem[j]

[a]Department of Molecular Biology and Microbiology, Tufts University School of Medicine, Boston, Massachusetts, USA
[b]Graduate Program in Immunology, Tufts Graduate School of Biomedical Sciences, Boston, Massachusetts, USA
[c]UMass Memorial Health Care, University of Massachusetts Medical School, Worcester, Massachusetts, USA
[d]Graduate Program in Molecular Microbiology, Tufts Graduate School of Biomedical Sciences, Boston, Massachusetts, USA
[e]Department of Anesthesiology, University at Buffalo School of Medicine, Buffalo, New York, USA
[f]Department of Immunology, Tufts University School of Medicine, Boston, Massachusetts, USA
[g]Department of Translational Medicine, Lund University, Malmö, Sweden
[h]Jean Mayer USDA Human Nutrition Research Center on Aging at Tufts University, Boston, Massachusetts, USA
[i]Stuart B. Levy Center for Integrated Management of Antimicrobial Resistance at Tufts (Levy CIMAR), Boston, Massachusetts, USA
[j]Department of Microbiology and Immunology, University at Buffalo School of Medicine, Buffalo, New York, USA

Basma H. Joma and Nalat Siwapornchai are co-first authors who contributed equally to this work; the order of their names is listed alphabetically.

ABSTRACT *Streptococcus pneumoniae* (pneumococcus) resides asymptomatically in the nasopharynx (NP) but can progress from benign colonizer to lethal pulmonary or systemic pathogen. Both viral infection and aging are risk factors for serious pneumococcal infections. Previous work established a murine model that featured the movement of pneumococcus from the nasopharynx to the lung upon nasopharyngeal inoculation with influenza A virus (IAV) but did not fully recapitulate the severe disease associated with human coinfection. We built upon this model by first establishing pneumococcal nasopharyngeal colonization, then inoculating both the nasopharynx and lungs with IAV. In young (2-month-old) mice, coinfection triggered bacterial dispersal from the nasopharynx into the lungs, pulmonary inflammation, disease, and mortality in a fraction of mice. In aged mice (18 to 24 months), coinfection resulted in earlier and more severe disease. Aging was not associated with greater bacterial burdens but rather with more rapid pulmonary inflammation and damage. Both aging and IAV infection led to inefficient bacterial killing by neutrophils *ex vivo*. Conversely, aging and pneumococcal colonization also blunted alpha interferon (IFN-α) production and increased pulmonary IAV burden. Thus, in this multistep model, IAV promotes pneumococcal pathogenicity by modifying bacterial behavior in the nasopharynx, diminishing neutrophil function, and enhancing bacterial growth in the lung, while pneumococci increase IAV burden, likely by compromising a key antiviral response. Thus, this model provides a means to elucidate factors, such as age and coinfection, that promote the evolution of *S. pneumoniae* from asymptomatic colonizer to invasive pathogen, as well as to investigate consequences of this transition on antiviral defense.

KEYWORDS coinfection, secondary bacterial pneumonia, *Streptococcus pneumoniae*, influenza A, colonization, aging, neutrophils, inflammation

Streptococcus pneumoniae (pneumococcus) is a Gram-positive pathobiont that typically resides asymptomatically in the nasopharynx (NP) of healthy individuals (1). It is hypothesized that *S. pneumoniae* establishes an asymptomatic biofilm on the

Citation Joma BH, Siwapornchai N, Vanguri VK, Shrestha A, Roggensack SE, Davidson BA, Tai AK, Hakansson AP, Meydani SN, Leong JM, Bou Ghanem EN. 2021. A murine model for enhancement of *Streptococcus pneumoniae* pathogenicity upon viral infection and advanced age. Infect Immun 89:e00471-20. https://doi.org/10.1128/IAI.00471-20.

Editor Nancy E. Freitag, University of Illinois at Chicago

Address correspondence to John M. Leong, john.leong@tufts.edu, or Elsa N. Bou Ghanem, elsaboug@buffalo.edu.

Received 28 July 2020
Returned for modification 6 September 2020
Accepted 10 May 2021
Accepted manuscript posted online 24 May 2021
Published 15 July 2021

nasopharyngeal epithelium by attenuating the production of virulence factors and concomitant inflammation (2–5). However, when immunity is compromised, a common occurrence in aging (6), pneumococci can cause serious disease such as otitis media, pneumonia, meningitis, and bacteremia (7). In humans, pneumococcal carriage is believed to be a prerequisite to invasive disease (8, 9). Bacterial isolates from invasive infections are genetically identical to those found in the nasopharynx of patients (9); this and other longitudinal studies have led to the suggestion that invasive disease often involves pneumococcal carriage in the upper respiratory tract (8, 9).

The rate of reported colonization is quite variable among adults and is confounded by differences in detection methods, but colonization may be more prevalent in the elderly (10). A meta-analysis of 20 nine published studies found that in individuals above 60 years of age, conventional culture showed 0 to 39% carriage, while 3 to 23% carriage was detected by molecular methods (11). Importantly, carriage was higher among nursing home residents (11). In older adults, conventional culture methods estimated carriage to be $<$5% (12–14), but more recent data from European studies using molecular detection methods indicated that carriage in the elderly ranges from 10 to 22% (10, 15–17). Thus, carriage rates may be much higher than what was previously estimated in elderly individuals (12–14).

Advanced age increases the risk of invasive pneumococcal disease and pneumococcal pneumonia (7). Aging is associated with immunosenescence, the overall decline in immunity that accompanies aging, as well as with inflammaging, a low-grade chronic inflammation that render the elderly more susceptible to pulmonary infections (18). Polymorphonuclear leukocytes (PMNs), also known as neutrophils, are a crucial determinant of age-related susceptibility to primary pneumococcal infection (19). These cells are required to control bacterial burden at the start of infection (20–22). However, aging is accompanied by impaired PMN antibacterial function (23, 24). In addition, aged hosts experience exacerbated PMN pulmonary influx during primary pneumococcal pneumonia (19, 25, 26), and persistence of PMNs in the airways beyond the first few days leads to tissue destruction and systemic spread of infection (27).

In addition to advanced age, epidemiological and experimental data show that invasive pneumococcal infections are strongly associated with viral infection (28–30). The risk of pneumococcal pneumonia is enhanced 100-fold by influenza A virus (IAV) infection (31, 32), resulting in the seasonal peak of pneumococcal disease during influenza outbreaks (32). Furthermore, *S. pneumoniae* is historically among the most common etiologies of secondary bacterial pneumonia following influenza and is associated with the most severe outcomes (29, 33–35). Symptoms of secondary bacterial pneumonia include cough, dyspnea, fever, and muscle aches, and when severe result in hospitalizations, respiratory failure, and mechanical ventilation and can lead to death (29, 33–35).

IAV commonly infects the upper respiratory tract, and at this location viral infection can enhance the nutritional environment for pneumococcus in the nasopharynx, leading to greater bacterial loads and/or higher rates of bacterial acquisition (4, 36). IAV can also directly bind the pneumococcal surface and enhance bacterial binding to the pulmonary epithelium leading to increased colonization (37). In addition, viral infection of the pulmonary epithelium induces the release of host components, such as ATP and norepinephrine, that are sensed by biofilm-associated pneumococci, triggering both the production of pneumococcal virulence factors and the dispersal of bacteria (4, 36, 38, 39). This in turn facilitates bacterial spread to and colonization of the lower respiratory tract (4).

IAV can infect not just the upper respiratory tract but also the lungs, and murine models featuring sequential pulmonary challenge with IAV first, followed by pneumococcus, show that the virus can compromise immune defense against pneumococcus (28, 33, 40). In these models, IAV alters both the pulmonary environment and the immune response to enhance subsequent bacterial colonization and tissue damage. For example, IAV preinfection increases mucus production and fibrosis and dysregulates ciliary

function (33, 41, 42), thus impairing mechanical clearance of invading bacteria. Viral enzymes, along with virus-elicited inflammation, result in the exposure of epithelial proteins that promote pneumococcal adherence to and invasion of host cells (40, 43–45). Furthermore, IAV triggers type I and II interferon (IFN) responses that impair both the recruitment and antibacterial function of phagocytes that are key to defense against pneumococcus (46–49). The combined tissue damage and the compromise in immune function render the lung more permissive for invasive *S. pneumoniae* infection (33, 44, 46). Less understood is how *S. pneumoniae* infection may alter host antiviral responses and viral replication in the lung.

Notably, advanced age and IAV infection appear to synergistically enhance susceptibility to pneumococcal lung infections (6, 18, 50; see also https://www.cdc.gov/flu/about/burden/index.html). Indeed, individuals ≥65 years old account for 70 to 85% of deaths due to pneumonia and influenza (https://www.cdc.gov/flu/about/burden/index.html). Interestingly, elderly individuals with influenza-like symptoms were reported to have an increased pneumococcal carriage rate of 30% (51). In animal models in which bacteria are directly instilled into the lungs following influenza infection, aging is associated with increase susceptibility of secondary pneumococcal pneumonia (50). Age-dependent changes in the expression of key components of innate immune signaling contribute to disease in this coinfection model (50). However, the factors that trigger the transition of pneumococci from benign colonizer to pathogen, including those that are age-dependent, are poorly defined, in part because small animal models that recapitulate the transition from asymptomatic colonization to overt clinical illness are lacking.

These above-described studies indicate that bacterial-viral synergy is multifactorial and can occur at different sites within the host. Insight into events that occur in both the nasopharynx and lung and contribute to the heightened susceptibility of the aged to serious disease upon pneumococcal/IAV coinfection is needed to develop better therapeutic and preventative approaches. A current murine model for the spread of nasopharyngeal pneumococci to the lung after viral infection of the upper respiratory tract relies on initial bacterial colonization of the nasopharynx followed by viral infection, but it does not recapitulate the severe signs of human clinical disease (4). Influenza virus is capable of infection not just of the upper respiratory tract, but also of the lung (52, 53). To better investigate the transition of *S. pneumoniae* from asymptomatic colonizers to invasive pathogens following IAV infection, as well as the effect of host age on the disease process, we built upon this mouse model of *S. pneumoniae*/IAV coinfection by incorporating viral infection of the lower respiratory tract. The enhanced model recapitulates the severe and age-exacerbated clinical disease observed in humans.

RESULTS

Intranasal IAV inoculation of mice precolonized with *S. pneumoniae* strain TIGR4 does not result in disease. Biofilm-grown *S. pneumoniae* cells are relatively less virulent and are thus adapted to host colonization rather than disease (2–4). A previously established murine model in BALB/cByJ mice utilizes biofilm-grown *S. pneumoniae* serotype 2 strain D39 and serotype 19F strain EF3030 to establish heavy carriage in the nasopharynx (4). Then, 2 days after bacterial inoculation, IAV is introduced into the nasal cavity and results in the spread of pneumococci from the nasopharynx (NP) to the lung (4). We first recapitulated this model with *S. pneumoniae* strain TIGR4, an invasive serotype 4 strain (54, 55) that we previously found to be highly virulent in aged C57BL/6 mice (19). We intranasally (i.n.) inoculated young (8- to 10-week-old) C57BL/6 (B6) mice with 1×10^6 CFU of biofilm-generated *S. pneumoniae* TIGR4 by delivering the bacteria in 10 μl of PBS (a volume that is unlikely to inoculate the lung [56]) to the nares of nonanesthetized mice. Forty-eight hours later, mice were inoculated i.n. with 10 μl of PBS containing 20 PFU of influenza A (IAV) virus PR8 (see Fig. S1A in the supplemental material for general scheme). Control groups of mice were infected with either *S. pneumoniae* or IAV alone. However, under these conditions, mice did not display signs of sickness, nor did bacteria spread into the lungs after 7 days (data not shown).

To increase the likelihood of clinical disease, we repeated the experiment with a 5-fold higher (5×10^6 CFU) dose of bacteria and a 25-fold higher dose (500 PFU) of IAV.

Similarly to earlier reports for other *S. pneumoniae* strains (D39 and EF3030) (4), IAV coinfection resulted in a 10-fold increase in *S. pneumoniae* TIGR4 in the nasal lavage fluid at 2 days post-IAV infection (Fig. S1B). In addition, IAV coinfection was associated with the detection of bacteria in the lungs of 40% of mice, compared to no detection in the control group infected with *S. pneumoniae* TIGR4 alone. This trend is consistent with the previous BALB/cByJ mice model of coinfection (4) but did not reach statistical significance. Furthermore, coinfection was not associated with weight loss when assessed over the course of 4 days postinfection (Fig. S1C). We also scored mice for clinical signs of the disease based on weight loss, activity, posture, and breathing and ranging from healthy (score = 0) to moribund (score = 25) and requiring euthanasia if the score was >9, as previously described (57). As secondary pneumonia can occur several days following IAV (40), we monitored the disease course up to 7 days, but did not detect disease symptoms or death in any of the coinfected mice (100% survival and a daily clinical score of 0 [including weight loss] for all mice). Therefore, despite promoting bacterial dispersal from the nasopharynx into the lungs, similarly to the previous work with other *S. pneumoniae* strains and BALB/c mice (4), this model of *S. pneumoniae* TIGR4/IAV coinfection did not result in overt clinical signs of disease.

Combined intranasal/intratracheal IAV inoculation of *S. pneumoniae*-colonized mice results in bacterial dissemination and disease. IAV infection is not restricted to the upper respiratory tract, and it can cause viral pneumonia in a significant fraction of infected individuals (52, 53) that is likely to be crucial for creating an environment in the lungs that is more permissive for bacterial infection (28, 33, 40). Indeed, viral lung infection diminishes pulmonary defenses against *S. pneumoniae* and promotes secondary bacterial pneumonia (33, 40, 43–49). Delivery of IAV i.n. to BALB/cByJ mice results in signs of viral pneumonia (4), but we found that pulmonary access of inocula delivered via the nasopharynx is more restricted in B6 mice compared to that in BALB/c mice (data not shown), raising the possibility that the lack of disease observed in coinfected B6 mice was due to the exclusive localization of virus in the nasal cavity, with limited opportunity to alter systemic or pulmonary immunity. In fact, when we measured pulmonary viral load at 2 days following i.n. infection with 500 PFU IAV, we were unable to detect any PFU in the lungs, while delivery of 20 PFU of IAV by intratracheal (i.t.) inoculation was sufficient to establish lung infection (see Fig. S2 in the supplemental material).

Therefore, to ensure delivery of IAV to both the nasopharynx and the lungs, we coinfected *S. pneumoniae*-colonized B6 mice by delivering the virus by two routes. Mice were inoculated i.n. with 5×10^6 CFU of biofilm-grown *S. pneumoniae* TIGR4 and infected 48 h later not only with 500 PFU IAV i.n., but also with 20 PFU i.t. to ensure pulmonary infection (Fig. 1A). No mice in a control group inoculated i.n. with *S. pneumoniae* alone lost weight (Fig. 1B), displayed clinical signs of sickness (Fig. 1C), or died (Fig. 1D). A second control group, inoculated i.n. and i.t. with IAV alone, displayed no disease until after day 4, when mice exhibited weight loss (Fig. 1B) and began succumbing to viral infection (Fig. 1D). In contrast, inoculation of IAV to animals precolonized with *S. pneumoniae* caused a bacterial/viral coinfection that resulted in weight loss (Fig. 1B), clinical symptoms (Fig. 1C), and death (Fig. 1D) that were detected starting day 2 post-IAV introduction. At this time point, a higher fraction of coinfected mice displayed signs of disease compared to that in controls infected with IAV only (55% versus 64%), and disease was more severe in mice that displayed clinical symptoms, although this did not reach statistical significance. In addition, the overall survival rate among coinfected mice was significantly lower than that of mice singly infected with *S. pneumoniae* alone (Fig. 1D). These signs of exacerbated disease were associated with significantly higher bacterial burdens in the nasopharynx, as well as with translocation of *S. pneumoniae* into the lung, compared to those in mice colonized with the bacteria or mice infected with IAV alone (Fig. 1E). These findings demonstrated that the new coinfection model leads to disease in a fraction of young healthy mice, which may increase the likelihood of detecting enhanced susceptibility in vulnerable hosts.

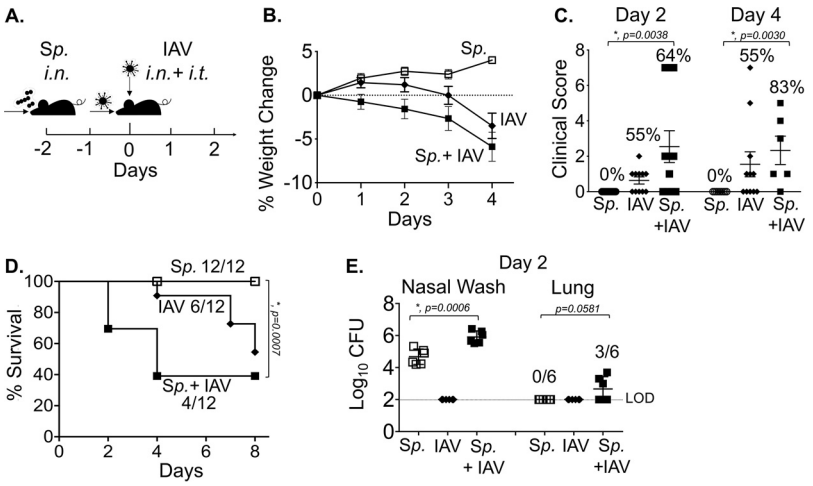

FIG 1 Combined intranasal/intratracheal influenza A virus (IAV) inoculation of *Streptococcus pneumoniae* (*Sp*)-colonized mice results in bacterial dissemination and disease. (A) Timeline of coinfection; 8- to 10-week-old male C57BL/6 (B6) mice were inoculated intranasally (i.n.) with 5×10^6 CFU of biofilm-grown *S. pneumoniae* TIGR4 to establish colonization in the nasopharynx. At 48 h later, the mice were either mock treated (*Sp*) or received 500 PFU of influenza A virus PR8 (IAV) i.n. and 20 PFU i.t. (B) Percent weight loss was monitored daily. (C) Blind clinical scoring was performed on day 2 and day 4 post IAV infection. The percentages denote the number of sick mice observed over the total number of mice. A score of 0 means no sign of sickness observed and a score greater than 1 indicates observable sickness. (D) Survival was monitored for 8 days post IAV infection, with fractions denoting the number of survivors over the total number of mice. (E) The bacterial burden in the nasopharynx and lung were determined at day 2 post IAV infection. Pooled data from four separate experiments are shown, in which one group of 12 mice in each experimental condition were monitored over time and another group of 6 mice per experimental condition were used for measuring bacterial burden. Statistically significant differences determined by Student's *t* test for bacterial burden and clinical score and by the log rank (Mantel-Cox) test for survival are indicated by asterisks. #, Statistical significance ($P < 0.05$) by Fisher's exact test between *Sp* and *Sp* plus IAV groups.

PMN depletion may have a small effect on the course of disease during IAV/*S. pneumoniae* coinfection. We previously found that in primary pneumococcal pneumonia, PMNs are required to control bacterial numbers early in the infection process; however, their persistence in the lungs is detrimental to the host and can promote the infection at later time points (20). To address the role of PMNs during coinfection, we treated young mice with PMN-depleting anti-Ly6G antibody (1A8) 1 day prior to pneumococcal colonization and throughout the coinfection (based on the timeline shown in Fig. 1A). We then confirmed that the cells were depleted by staining with the RB6 antibody followed by flow cytometry (see Fig. S3 in the supplemental material). Following infection, we measured bacterial burden, weight loss, clinical score, and survival over time. PMN depletion had no effect on bacterial burdens in the nasopharynx or on bacterial spread to the lungs or blood following coinfection (Fig. 2A and B). However, PMN-depleted mice appeared to lose more weight at days 3 and 4 post coinfection compared to the control group (Fig. 2C), and a greater proportion of PMN-depleted mice displayed clinical signs of sickness compared to the control group at both 18 h and 48 h post IAV infection (Fig. 2D). Additionally, lower survival was observed in the PMN-depleted group, in which 25% survived to day 7, compared to ~43% in the untreated control group (Fig. 2E). These differences did not reach statistical significance, but raise the possibility that PMNs provide a measure of defense to coinfection in young mice.

Aging increases susceptibility to IAV/*S. pneumoniae* coinfection. We next tested if the new coinfection mouse model (Fig. 1A) recapitulates the age-associated increase in susceptibility to secondary pneumococcal pneumonia. Aged (18- to 24-month-old) B6 mice were inoculated i.n. with 5×10^6 CFU of biofilm-grown *S. pneumoniae* TIGR4, and 48 h later were infected with 500 PFU IAV i.n. plus 20 PFU i.t. Compared to young coinfected controls, old mice displayed significantly more severe signs of disease, as indicated by a higher average clinical score (Fig. 3A). While seven of 16 (~44%) young

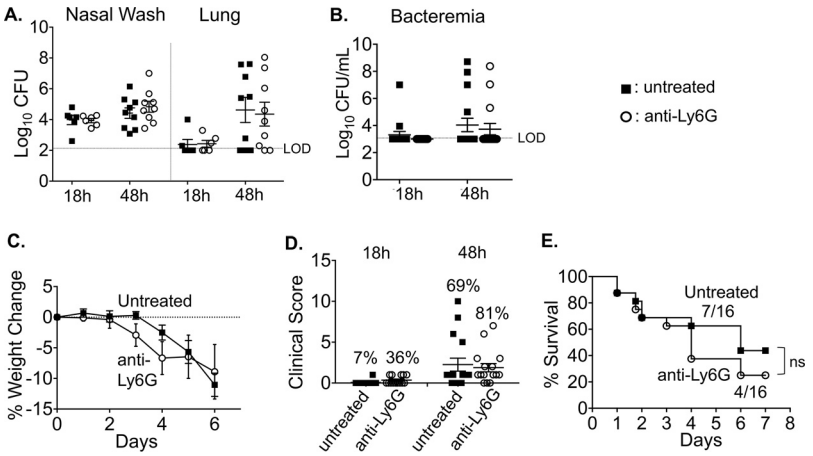

FIG 2 Polymorphonuclear leukocyte (PMN) depletion may have a small effect on the course of disease during IAV/*S. pneumoniae* coinfection. C57BL/6 mice (8 to 10 weeks old) were intraperitoneally (i.p.) injected with anti-Ly6G (clone 1A8) antibodies to deplete neutrophils or were mock treated. The antibodies were given daily from day −3 to day 1, and every other day from day 3 to the end of each experiment (with respect to IAV infection). (A) At 18 and 48 h post IAV infection, bacterial numbers in the nasal wash and lungs were determined. Pooled data from three separate experiments, with totals of $n = 6$ mice per experimental condition at 18 h and $n = 9$ mice per condition at 48 h, are shown. Bacteremia (B) and weight loss (C) were monitored over time. (D) Mice were scored in a blind manner for symptoms of diseases at 18 and 48 h post IAV-infection. The percentages indicate the number of mice with clinical sickness (clinical score above 1) over the total number of mice. (E) Survival was monitored over time; the fractions denote the number of survivors over the total number of mice at 8 days post IAV infection. (C to E) Data are pooled from three separate experiments, with $n = 16$ mice per group. Statistically significant differences were determined by Student's *t* test for bacterial burden and clinical score and by the log-rank (Mantel-Cox). ns, not significant.

mice showed clinical symptoms (i.e., a clinical score greater than 1; Fig. 3A), all 13 old mice showed at least some degree of illness by day 2 post coinfection ($P = 0.0012$; Fisher's exact test). Furthermore, whereas only 25% (4 out of 16) young mice had a clinical score greater than 2, which is indicative of more severe disease, 92% (12 out of 13) aged mice fell into this category ($P = 0.005$; Fisher's exact test). In addition, old mice died at a significantly accelerated rate. By day 2 post coinfection, 60% of old mice had succumbed to the infection, compared to only 25% of young mice. Differences in survival were observed at each successive time point, and at the end of the experiment on day 8, only 14% of old mice remained alive, compared to 50% of young mice (Fig. 3B). Importantly, the accelerated death observed in coinfected old mice was not observed in old mice infected with *S. pneumoniae* alone or with IAV alone (see Fig. S4 in the supplemental material).

We next tested whether these differences could be attributed to increased bacterial loads in the nasopharynx, lungs, or blood. As old mice got sicker at earlier time points after IAV coinfection, with the majority succumbing by day 4, we compared bacterial burden across age groups at 18 and 48 h after IAV coinfection. We found no significant differences in the numbers of pneumococci in nasopharyngeal washes, pulmonary homogenates, or blood at either time point (Fig. 3C to E). Taken together, these findings suggest that with aging there is an increased susceptibility to coinfection and an accelerated course of disease that could not be attributed to a more rapid bacterial dissemination or to higher bacterial loads in the nasopharynx, lung, or bloodstream.

Aging is associated with more rapid lung inflammation. To determine if the accelerated rate of death examined in coinfected old mice was due to more lung damage, we analyzed hematoxylin and eosin (H&E)-stained lung sections for alveolar congestion, hemorrhage, alveolar thickness, neutrophils, and lymphocytic infiltration (Fig. 4A). We found that the alveolar spaces of both uninfected old and young mice were clear and free of inflammatory or red blood cells (Fig. 4A). At 18 h post coinfection, the lungs of young mice did not show any overt signs of disease (Fig. 4A). In contrast,

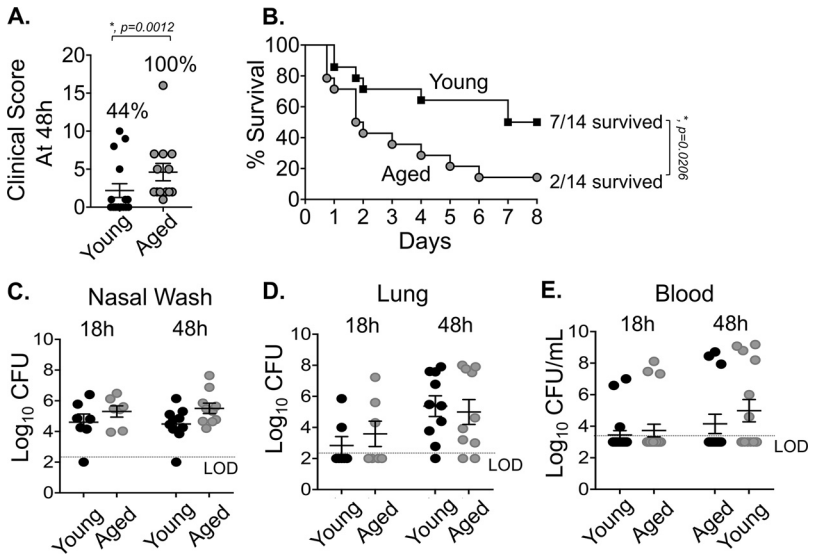

FIG 3 Aging increases susceptibility to IAV/*S. pneumoniae* coinfection. Young (8- to 10-week-old) and aged (18- to 24-month-old) C57BL/6 male mice were coinfected with *S. pneumoniae* TIGR4 i.n. and influenza A virus PR8 i.n. and i.t. (as shown in Fig. 1A). (A) Clinical score of coinfected young and aged mice at day 2 post IAV infection is shown; the percentage of mice with demonstrable illness is indicated. #, Statistical significance by Fisher's exact test. (B) Survival of coinfected young and aged mice were monitored over time, with fractions denoting the number of survivors over the total number of mice. Data are pooled from four experiments, with $n = 14$ mice per group. Asterisks indicate statistical significance by the log rank (Mantel-Cox) test. (C to E) Bacterial burdens in the nasal wash, lungs, and blood were determined at 18 and 48 h post IAV inoculation. The mean ± standard error of the mean pooled from three separate experiments are shown with $n = 7$ mice per condition at 18 h and $n = 10$ mice per condition at 48 h. LOD, limit of detection. For clinical score (A), data shown are pooled from all mice from experiments shown in panels B to E that had survived up to that time point (i.e., $n = 13$ for old and $n = 16$ for young).

coinfected old mice had significant lung pathology by 18 h postinfection, including a loss of alveolar architecture, and spotty inflammation consisting of infiltrates composed of neutrophils, alveolar macrophages, and mononuclear cells that were mixed with red blood cells (Fig. 4A). At 48 h postinfection, there were clear signs of lung pathology in both young and old coinfected mice (Fig. 4A).

Next, we tested the levels of inflammatory cytokines in coinfected young mice versus those in old mice. No significant differences between age groups were detected in baseline (uninfected) levels of any of the cytokines tested between the age groups (Fig. 4B and data not shown). However, consistent with the enhanced PMN influx at 18 h postinfection in aged mice, old mice had significantly higher levels of interleukin 10 (IL-10), IL-2, IL-1β, and tumor necrosis factor alpha (TNF-α) (Fig. 4B) compared with those in young mice. Levels of IL-12p70, IL-17, IL-6, and IFN-γ, were slightly but not significantly elevated at 18 h post coinfection (see Fig. S5A in the supplemental material). By 48 h, there were no significant differences between young and old mice in cytokine levels except for that of IFN-γ, which was higher in young mice (Fig. S5B).

We previously found that mice suffering from exacerbated PMN-mediated pulmonary inflammation during pneumococcal pneumonia did not display higher bacterial burdens in their lungs (27), despite a higher likelihood of severe disease (19, 20, 27). To test whether PMN influx was also higher in old coinfected mice, we measured the percentage and number of pulmonary PMNs ($Ly6G^+$) by flow cytometry. We found that old mice had significantly (6-fold) higher percentages and numbers of PMNs in their lungs compared to those of young controls at 18 h post coinfection (Fig. 4C). By 48 h, most aged mice had succumbed to the infection (Fig. 3B), confounding interpretation of PMN numbers at this time point; PMN percentages and numbers appeared to be higher in young mice, but the differences were not statistically significant (Fig. 4C). Macrophages, which are important for host resistance to *S. pneumoniae*/IAV

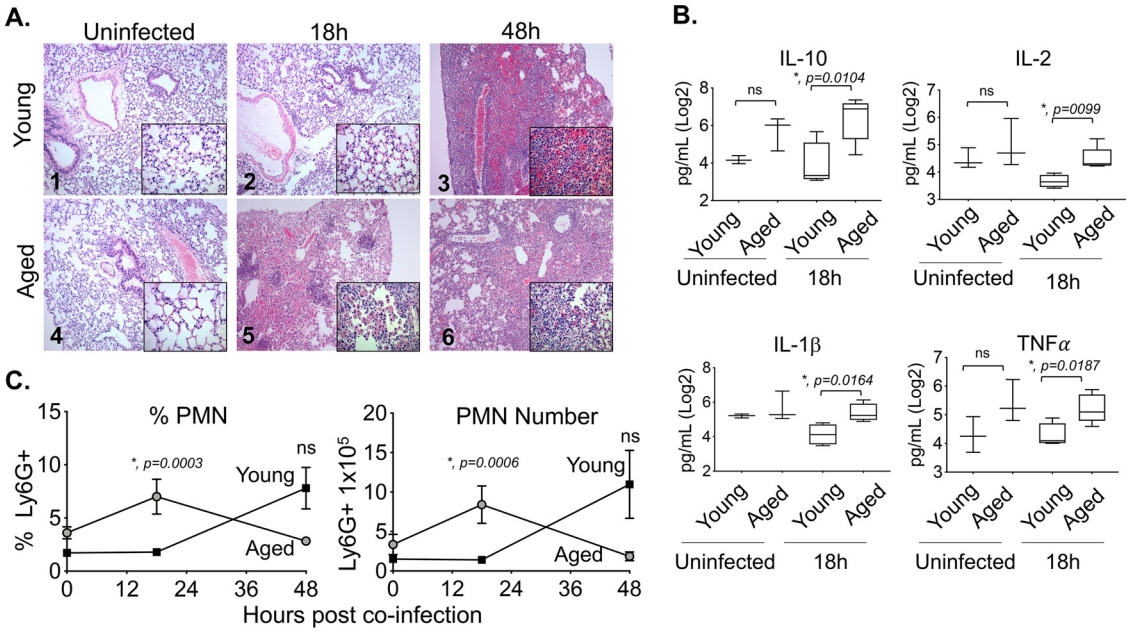

FIG 4 Aging is associated with more rapid lung inflammation. Young and aged C57BL/6 male mice were coinfected with *S. pneumoniae* and influenza A virus PR8. At 18 and 48 h following IAV infection (see experimental design in Fig. 1A), the lungs were harvested. (A) Lungs were stained with hematoxylin and eosin (H&E); shown are representative photographs at ×100 or ×400 (inset). (B) Cytokines in the supernatants of lung homogenates of young ($n = 4$) or aged ($n = 5$) mice at 18 h post coinfection were measured by multiplex enzyme-limited immunosorbent assay (ELISA). Asterisks represent statistical significance by Student's *t* test. (C) The percentages and total numbers of PMNs ($Ly6G^+$) in the lungs were measured by flow cytometry. Young mice are represented by open bars and aged mice by shaded bars. The mean ± SEM pooled from three separate experiments is shown where data are pooled from 12 mice per age group, except for 48 h post coinfection, at which point, due to the kinetics of disease, data from only 7 surviving old mice are shown. Statistically significant differences determined by Student's *t* test are indicated by asterisks.

coinfection (48) and display age-driven changes (58, 59), displayed no significant age-dependent differences in either percentage or number at 18 or 48 h after infection (see Fig. S6 in the supplemental material). Taken together, these findings demonstrate that aging is associated with earlier pulmonary inflammation and damage following coinfection, which may contribute to the accelerated death observed in this mouse group.

Aging and IAV infection diminish the ability of PMNs to kill *S. pneumoniae ex vivo*. Aged, coinfected mice experience an accelerated rate of pulmonary inflammation, but bacterial loads in the lungs of aged mice were not lower than those in young mice, indicating that PMN infiltration is not associated with bacterial clearance. Both aging (24) and IAV infection (60) have been reported to diminish the antibacterial function of PMNs. To assess the ability of PMNs to kill *S. pneumoniae* in our coinfection model, we used a well-established opsonophagocytic (OPH) killing assay (19, 61). We first compared the bactericidal activity of bone marrow-derived PMNs from young or aged mice. The percentage of bacteria killed upon incubation with PMNs for 45 or 90 min was determined by comparing surviving CFU to no-PMN control reactions at the same time point. We found that, as previously reported for humans (23) and mice (24), the ability of PMNs isolated from uninfected old mice to kill pneumococci was reduced 5-fold compared to that of young controls, regardless of the duration of infection (Fig. 5).

We next examined the bactericidal activity of PMNs isolated from young or old mice 2 days after i.t./i.n. IAV inoculation. As previously reported (46–49), PMNs from young IAV-infected mice had a slight (2-fold) but significant reduction in their ability to kill pneumococci compared to that of PMNs from uninfected controls (Fig. 5). Strikingly, IAV infection diminished the ability of PMNs from old mice to kill *S. pneumoniae*; instead, PMNs from IAV-infected old mice promoted a slight increase in bacterial numbers (Fig. 5). These findings suggest that IAV infection completely abrogates the ability of PMNs from old mice to kill *S. pneumoniae*.

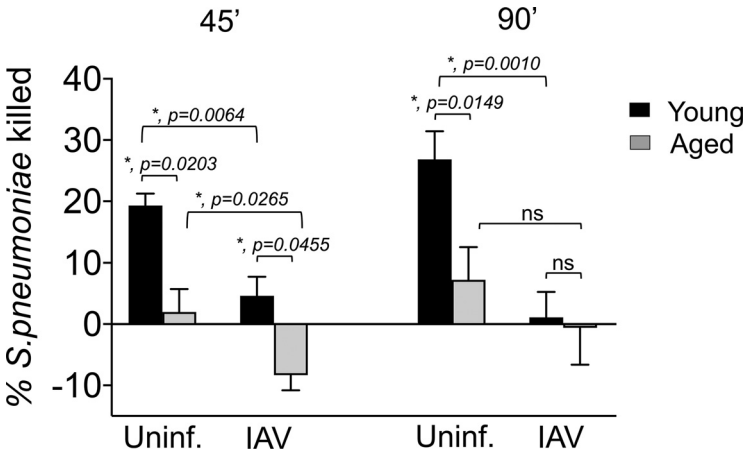

FIG 5 Aging and IAV infection diminish the ability of PMNs to kill *S. pneumoniae ex vivo*. PMNs were isolated from the bone marrow of young (8- to 10-week-old) and aged (18- to 24-months-old) C57BL/6 male mice that were mock infected (uninf.) or singly infected with IAV (i.n. + i.t.) for 2 days. PMNs were incubated with *S. pneumoniae* preopsonized with homologous serum from the same mouse for 45 or 90 min at 37°C. The percentages of *S. pneumoniae* killed upon incubation with PMNs were determined with respect to a no-PMN control. Data shown represent the means ± SEM pooled from two experiments ($n = 3$ mice per group per time point), where each condition was tested in quadruplicates per experiment. Asterisks represent statistical significance as determined by Student's *t* test.

Aging and prior colonization with *S. pneumoniae* result in impaired IFN-α production and higher viral burden in the lungs. Finally, we investigated whether aging and/or bacterial coinfection had an impact on antiviral responses. Old or young B6 mice were inoculated i.n. with 5×10^6 CFU of biofilm-grown *S. pneumoniae* TIGR4 or were mock challenged with phosphate-buffered saline (PBS) and 48 h later were infected with 500 PFU IAV i.n. and 20 PFU i.t. At 48 h following viral infection, we compared viral burden in the lung across age groups. We found that bacterial colonization resulted in 10-fold (and statistically significant) higher pulmonary viral loads compared to those of mock-colonized controls, regardless of host age (Fig. 6A). Furthermore, we found that in coinfected hosts, aging was associated with significantly increased viral loads in the lungs (Fig. 6A), suggesting that enhanced viral loads and impaired antiviral defenses contribute to the differences in clinical manifestation across host age.

To test whether bacterial colonization and aging impair antiviral immune responses, we measured the levels of IFN-α, a cytokine crucial for antiviral defense (62). We found that in young mice, despite the higher viral burden (Fig. 6A), prior bacterial colonization resulted

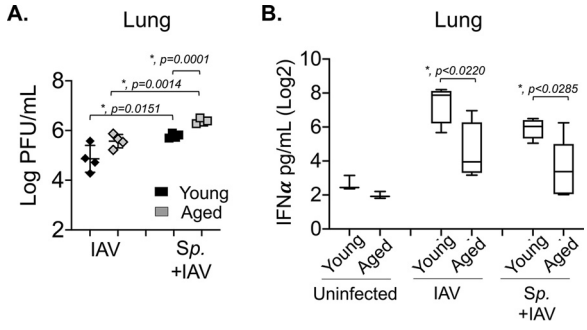

FIG 6 Aging and prior colonization with *S. pneumoniae* result in impaired IFN-α production and higher viral burden in the lungs. Young and aged C57BL/6 male mice were either coinfected with *S. pneumoniae* and influenza A virus PR8 (*Sp* + IAV), challenged with virus alone (IAV), or mock challenged with phosphate-buffered saline (PBS) (uninfected) (as in Fig. 1A). At 2 days post IAV-infection, (A) viral burdens in the lungs were determined and (B) levels of IFN-α in the supernatants of lung homogenates were measured by ELISA. Data from $n = 4$ mice per group are shown. Statistically significant differences were determined by Student's *t* test.

in a 3-fold (but not statistically significant) decrease in IFN-α production in the lungs in response to IAV challenge (Fig. 6B). Notably, aging was associated with (statistically significant) 5- and 3-fold lower levels of IFN-α in mice infected with IAV alone or coinfected with IAV and *S. pneumoniae*, respectively. No differences in IFN-α production were observed in the sera (see Fig. S7 in the supplemental material). These findings suggest that both pneumococcal infection and aging blunt antiviral responses in this mouse model.

DISCUSSION

S. pneumoniae remains a leading cause of secondary bacterial pneumonia following influenza A virus infection and is associated with severe disease (29, 33–35), particularly in the elderly (https://www.cdc.gov/flu/about/burden/index.html). The majority of *S. pneumoniae*/IAV coinfection experimental studies have delivered bacteria into the lungs of mice preinfected with IAV to reveal changes in the host lungs and immune response that are crucial for priming invasive pneumococcal disease (33, 40, 43–49). In this study, to investigate the transition of *S. pneumoniae* from colonizer to pathogen upon IAV coinfection, a process that has just started to be elucidated (4, 36), we developed a modified murine infection model that recapitulates this transition and results in severe clinical disease. In a previously established model, female BALB/cByJ mice were first colonized intranasally with biofilm-grown pneumococci and then infected with IAV by delivering the virus to the nasopharynx (4, 39). This model showed that changes in the host environment in response to viral infection triggers the dispersal of pneumococci from colonizing biofilms and their spread to the lower respiratory tract (4). Importantly, the dispersed bacteria expressed higher levels of virulence factors required for infection, thus, rendering them more highly pathogenic (4). Nevertheless, upon dispersion following *in vivo* IAV infection, although bacterial migration to the lung was detected, the burden was less than 100 CFU per lung, and the mice did not suffer overt disease. When we used this model to coinfect male C57BL/6 (B6) mice, we also observed a significant increase in dispersed bacteria in the nasopharynx, but no disease and only a transient presence of *S. pneumoniae* in the lungs of B6 mice. Here, we performed experiments in male instead of female mice due to both the easier availability of aged male animals and the documented higher rate of pneumococcal pneumonia in men compared to that in women (63, 64).

Previous work on pneumococcal inoculation of IAV-infected lungs showed viral infection to be crucial for creating an environment in the lungs that is more permissive for bacterial infection (40, 43–49). The relatively low bacterial burden in coinfected male B6 mice observed here upon IAV inoculation by the i.n. route alone suggested that the lung environment was not sustaining the bacteria. It is possible that human IAV/*S. pneumoniae* coinfection involves viral infection of not only the upper respiratory tract, but the lower respiratory tract as well (52, 53). Therefore, we coinfected *S. pneumoniae*-colonized B6 mice with IAV by delivering the virus not only i.n. to infect the nasopharynx but also i.t. to ensure infection of the lungs. This modified model recapitulated the increase in nonadherent pneumococci in the nasopharynx observed upon viral coinfection (4, 65, 66) and resulted in bacterial spread into the lungs and circulation that increased over time. Importantly, this mode of dual infection recapitulated both the increased colonization burden (67, 68) and the clinical signs of severe disease observed in humans (29, 33–35), and it resulted in death of approximately half of the coinfected young controls.

Although the elderly are at a higher risk for secondary pneumococcal pneumonia following IAV infection, animal studies exploring this age-driven susceptibility to coinfection are few (50, 69, 70). Here, using the modified model, we found that old mice were significantly more susceptible to *S. pneumoniae*/IAV coinfection. Old mice displayed more severe signs of disease compared to young controls, and the majority ($>$85%) failed to survive the coinfection. This increased susceptibility in old mice was not linked to higher bacterial dissemination from the nasopharynx, greater establishment of infection in the lungs, or systemic spread into the circulation at the time points tested. Susceptibility to viral infection alone, as measured by weight loss within the

first 5 days following IAV, was also similar between the age groups. Rather, the age-driven susceptibility to coinfection was associated with earlier and more severe pulmonary inflammation. Production of pulmonary cytokines is elevated in young mice infected with *S. pneumoniae* at 7 days after IAV inoculation (71). Furthermore, old mice display changes in the expression of pattern recognition receptors in the lungs, which lead to altered inflammatory responses (50). Similarly to previous studies (50), we found here that coinfected old mice had higher levels of TNF-α compared to those of young controls. However, in contrast to previous reports that found reduced NLRP3 inflammasome expression in the lungs and lower production of IL-1β, we found higher levels of IL-1β in old versus young mice. This may be accounted for by differences in expression of bacterial factors. The expression of pneumolysin, which was found to activate NLRP3 inflammasomes and lead to production of IL-1β (72), was elevated in pneumococci dispersed from biofilms upon IAV infection (73) and therefore may have primed the IL-1β production we observed in old mice.

We previously found that PMNs were key determinants of disease during primary pneumococcal pneumonia and are required to initially control bacterial numbers (20, 74). Therefore, we explored here the role of PMNs in *S. pneumoniae*/IAV coinfection. Similarly to other studies, we found that PMNs are recruited to the lungs of coinfected young mice (48). Previous reports indicate that the PMN-mediated antipneumococcal function in IAV-infected mice (60) and humans (68) is progressively reduced over time. For example, in mice, PMNs demonstrably contribute to host defense at 3 days but not at 6 days postinfection (60). Nevertheless, PMN depletion showed that these cells are important for control of bacterial transmission (75) and control of pulmonary bacterial numbers (48) in IAV coinfected mice. Similarly, we found here that PMN depletion starting prior to bacterial colonization and continuing throughout viral coinfection appeared to slightly worsen disease progression, with slightly greater average weight loss at days 3 and 4 after viral inoculation and a greater proportion of PMN-depleted mice succumbing to coinfection. However, PMN depletion had no significant effect on the number of dispersed *S. pneumoniae* bacteria in the nasopharynx or on their spread to the lungs and blood. It is possible that, in this model, IAV may rapidly impair PMN function, limiting their efficacy even in PMN-replete mice. In fact, we found that within 2 days following IAV infection, the ability of bone marrow-derived PMNs to kill *S. pneumoniae* was significantly blunted in young mice. Alternatively, the apparent inability of PMNs to limit bacterial numbers in this model could be due to the enhanced virulence of pneumococci dispersed from the nasopharyngeal environment (4) compared to that of the broth-grown bacteria typically used in other models (60).

Here, we found that aging was associated with earlier influx of PMNs into the lungs of coinfected mice. We previously demonstrated that excessive PMN influx into the lungs is detrimental for the ability of old mice to control invasive disease following primary pneumococcal pneumonia (19) and that PMN depletion 18 h after infection boosted host survival (20). Similarly, greater PMN influx into the lungs of old mice singly infected with IAV was associated with host mortality, and depletion of these cells 6 days following viral infection significantly boosted host survival (76). Uncontrolled PMN influx can result in tissue damage, disruption of gaseous exchange, and pulmonary failure. In fact, it was reported that in old mice singly infected with IAV, PMNs enhanced lung inflammation and damage, and their depletion reduced the levels of inflammatory IL-1β and TNF-α (76). Therefore, the early increase in these inflammatory cytokines and lung damage that we observed here in *S. pneumoniae*/IAV-coinfected old mice may be driven by the elevated levels of pulmonary PMNs.

The age-associated increased levels of pulmonary IL-10 during *S. pneumoniae*/IAV coinfection that we observed here may also contribute to the enhanced susceptibility of old mice to coinfection. IL-10 levels are elevated in coinfected young mice compared to those singly infected with *S. pneumoniae* (77). We showed that blocking this cytokine boosts PMN antibacterial function by inhibiting reactive oxygen species (ROS) production (74), and van der Poll and coworkers demonstrated that

inhibition of IL-10 restores resistance of vulnerable hosts to primary pneumococcal pneumonia (77).

The more severe disease observed in old mice also correlated with higher viral lung burden during both coinfection with *S. pneumoniae* and IAV and single infection with IAV, although the difference reached statistical significance only in the former. Production of type I IFN, which is crucial for control of viral replication, is dysregulated during aging (78), and we found that pulmonary IFN-α levels of coinfected or singly infected old mice were significantly lower than those of their young counterparts. Hence, in this model, enhanced disease associated with aging may be a reflection of a combination of an exuberant PMN response and a muted type I interferon response.

While many studies have examined the effect of IAV on secondary pneumococcal pneumonia, the effect of bacterial colonization on viral infection has been less explored. We found that, regardless of host age, prior colonization with pneumococci resulted in significantly higher viral pulmonary loads. In experiments involving two different hosts (ferrets or cotton rats) and two different viruses (IAV and human respiratory syncytial virus [RSV], respectively), nasopharyngeal colonization of donors with *S. pneumoniae* promoted viral transmission (79, 80). In the latter (rat-RSV) model, prior pneumococcal colonization enhanced viral infection of the upper respiratory tract but did not promote infection of the lungs (80). A human experimental pneumococcal colonization study showed that prior colonization with pneumococci did not increase the burden of a live attenuated influenza virus, but reduced proinflammatory immune responses in the nasopharynx and significantly blunted antiviral IgG production in the lungs (81). Hence, prior colonization with pneumococci may impair antiviral defenses. Indeed, we found that in spite of their approximately 1 log higher viral lung burden compared to that of singly infected mice, *S. pneumoniae*-precolonized young and old mice displayed 5-fold and 3-fold lower levels of pulmonary IFN-α, respectively, than those of noncolonized controls.

In summary, we modified existing murine models to establish an experimental system that reflects the transition of *S. pneumoniae* from asymptomatic colonizer to invasive pulmonary pathogen upon IAV coinfection. In this model, IAV triggers the transition of a pathobiont from a commensal to a pathogenic state through modification of bacterial behavior in the nasopharynx, enhancement of bacterial colonization in the lung, and compromise of PMN-mediated antibacterial immunity. In turn, pneumococci modulate antiviral immune responses and promote IAV infection of the lower respiratory tract. Importantly, this model recapitulates the susceptibility of aging to coinfections. Moving forward, this multistep model can be used to dissect both the multiple phases of pneumococcal disease progression from commensals to pathogens and the complexity of viral/bacterial interactions within different hosts, thus helping inform specialized treatment options (65) tailored to the susceptible elderly population.

MATERIALS AND METHODS

Mice. Young (8- to 10-week-old) and aged (18- to 24-month-old) male C57BL/6 mice were purchased from Jackson Laboratories (Bar Harbor, ME) and the National Institute of Aging. Mice were housed in a pathogen-free facility at Tufts University. All procedures were performed in accordance with Institutional Animal Care and Use Committee guidelines. The number of mice included in each experiment was based on power analysis. At least 6 mice per group for determination of bacterial burden and 12 mice per group for monitoring survival were included to sufficiently power our studies. In each experiment, an equal number of mice per group were planned. However, slight variations in the number of mice per group at later time points of several experiments occurred due to the required euthanasia of several mice in highly susceptible experimental groups.

Bacterial biofilms. NCI-H292 mucoepidermoid carcinoma (H292) cells were grown in 24-well plates in RPMI 1640 medium with 10% fetal bovine serum (FBS) and 2 mM L-glutamine until confluence. Cells were washed with 1× PBS and fixed in 4% paraformaldehyde for 1 h on ice. *S. pneumoniae* TIGR4 cells (a kind gift from Andrew Camilli) were grown on tryptic soy agar plates supplemented with 5% sheep blood agar (blood agar plates) overnight, then diluted and grown in chemically defined liquid medium (CDM) (4, 39) supplemented with Oxyrase until an optical density at 600 nm (OD_{600}) of 0.2. Bacteria were diluted 1:1,000 in CDM and seeded on the fixed H292 cells. Then, bacteria/H292 cells were incubated at 34°C/5% CO_2 and medium was changed every 12 h. At 48 h postinfection, the supernatant containing

planktonic (nonadherent to NCI-H292 cells) bacterial cells was discarded, the cells gently washed with PBS, and adherent biofilms collected in fresh CDM by vigorous pipetting. Biofilm aliquots were then frozen at −80°C in the CDM with 25% (vol/vol) glycerol.

Intranasal inoculation. Before use, biofilm aliquots were thawed on ice, washed once, and diluted in PBS to the required concentration. The mice were restrained without anesthesia and infected i.n. with 10 μl (5×10^6 CFU) of biofilm-grown *S. pneumoniae*. The inoculum was equally distributed between the nostrils with a pipette. This method of inoculation results in pathogen delivery limited to the nasal cavity, without accessing the lower tract in C57BL/6 mice (56). Bacterial titers were confirmed by serial dilution and plating on blood agar plates. To ensure stable colonization of the biofilm in the nasopharynx, groups of mice were euthanized at 18 and 48 h postinoculation, and the nasal washes and tissue were collected and plated on blood agar plates for enumeration of *S. pneumoniae*.

Viral infection. The mouse-adapted H1N1 Influenza A virus PR8 (A/PR/8/34) was obtained from Bruce Davidson (4, 39) and stored at −80°C. Before use, viral aliquots were thawed on ice, diluted in PBS, and used to inoculate mice. At 48 h following bacterial inoculation, mice were infected i.n. with 10 μl of 500 PFU of virus by pipetting the inoculum into the nostrils of nonanesthetized mice. Following i.n. inoculation, mice were lightly anesthetized with isoflurane and challenged i.t. with 20 PFU of virus in a 50-μl volume pipetted directly into the trachea, with the tongue pulled out to facilitate delivery (20).

Clinical scoring and bacterial burden. Following coinfection, mice were monitored daily and scored in a blind manner for signs of sickness, which included weight loss, activity, posture, and breathing. Based on these criteria, the mice were given a clinical score of healthy (0) to moribund (25), modified from a previous description (57). Any mice displaying a score greater than 9 were humanely euthanized in accordance with our protocol. Mice were euthanized at indicated time points, and the lung, nasal lavage, and blood samples collected and plated on blood agar for enumeration of bacterial loads, as previously described (20). For collection of serum, blood was collected via cardiac puncture into Microtainer tubes (BD Biosciences) and centrifuged at 7,607 $\times$ *g* for 2 min to collect serum per the manufacturer's instructions.

Depletion of PMNs. Mice were intraperitoneally (i.p.) injected with 100 μl (50 μg/mouse) of anti-Ly6G clone 1A8 (BD Biosciences) to deplete neutrophils. Mice were injected daily with the depleting antibodies starting 1 day prior and ending 2 days after bacterial inoculation, followed by every other day from day 1 after viral coinfection to the end of each experiment. Treatment resulted in >90% neutrophil depletion, as described below.

Cell isolation and flow cytometry. Mouse lungs were harvested, washed in PBS, and minced into small pieces. The sample was then digested for 45 min with RPMI 1640 1× supplemented with 10% FBS, 1 mg/ml type II collagenase (Worthington, Lakewood, NJ), and 50 U/ml DNase I to obtain a single-cell suspension, as previously described (20). The red blood cells were lysed using ACK lysis buffer (Gibco). Cells were then stained with anti-mouse Ly6G clone 1A8 (BD Biosciences), F480 clone BM8 (BioLegend), CD11c clone N418 (eBioscience), and CD11b clone M1/70 (eBioscience). For neutrophil depletion, cells isolated from the lungs at 18 and 48 h post coinfection were also stained with either Ly6G clone 1A8 or RB6 clone RB6-8C5 (BioLegend) antibodies to confirm cell depletion. The fluorescence intensities were measured on a BD LSR II flow cytometer at the Tufts Flow Cytometry Core Facility (Boston, MA) to capture at least 25,000 cells and were analyzed using FlowJo.

Isolation of PMNs and opsonophagocytic killing assay. Femurs and tibias of uninfected mice were collected and flushed with RPMI supplemented with 10% FBS and 2 mM EDTA to obtain bone marrow cells. Neutrophils were isolated by density gradient centrifugation using Histopaque 1119 and Histopaque 1077, as previously described (82). The neutrophils were resuspended in Hanks' (Gibco) buffer/0.1% gelatin with no Ca^+ or Mg^+ and tested for purity by flow cytometry using anti-Ly6G antibodies (eBioscience), where 85 to 90% of enriched cells were Ly6G-positive ($Ly6G^+$). The ability of neutrophils to kill bacteria was measured using a well-established opsonophagocytic (OPH) killing assay, as previously described (20). Briefly, 2.5×10^5 neutrophils were incubated in Hanks' buffer/0.1% gelatin with 10^3 CFU of *S. pneumoniae* preopsonized with 3% mouse sera. The reaction mixtures were incubated in flat-bottomed 96-well nonbinding plates for 45 min at 37°C. Each group was plated on blood agar to enumerate viable CFU. Percent bacterial killing was calculated in comparison to a no-PMN control under the same conditions.

Histology. Whole lungs were harvested from groups of mice at 18 h and at 48 h post coinfection and fixed in 10% neutral buffered formalin for 2 days. The tissues were then embedded in paraffin, sectioned at 5 μm, and stained with hematoxylin and eosin at the Animal Histology Core at Tufts University. Sections of lung from three mice per group were imaged using a Nikon Eclipse E400 microscope. Photomicrographs were captured using a SPOT Idea 5.0-megapixel color digital camera and SPOT software. Histopathologic scoring was performed by a board-certified anatomic pathologist experienced in murine pathology, from 0 (no damage) to 4+ (maximal damage) for alveolar congestion, hemorrhage, alveolar thickness, neutrophils, and lymphocytic infiltration (83).

Cytokine analysis. Frozen lung homogenates and serum samples were thawed on ice and mixed by gentle vortexing. Cytokines in the lung and serum samples were measured using the Mouse Cytokine 8-Plex array (Quanterix, Billerica, MA) following the manufacturer's instructions. Levels in lung supernatants and serum samples were measured using the CiraScan system at the Imager at Tufts University Genomic Core (Boston, MA) and analyzed by the CiraScan/Cirasoft program. Qlucore Omics Explorer (version 3.5) was used for the generation of lung cytokine box plots. Concentrations of cytokines (IL-10, IL-2, IL-1β, TNF-α, IL-6, IFN-γ, IL-17, and IL-12p70) were log transformed and displayed as Log_2 pg/ml. IFN-α was measured using the mouse IFN-α enzyme-limited immunosorbent assay (ELISA) kit (R&D Systems, MN, USA) following the manufacturer's instructions.

Plaque assay. Madin-Darby canine kidney (MDCK) cells were grown overnight in 12-well plates at 2×10^5 cells/well in Dulbecco's modified Eagle's medium (DMEM) plus 10% FBS. Cells were washed twice with 1× PBS and incubated with serial dilutions of viral inoculum or lung homogenates in DMEM supplemented with 0.5% low-endotoxin bovine serum albumin (BSA; Sigma-Aldrich) for 50 min in an incubator at 37°C with 5% CO_2. The plates were shaken every 10 min during the incubation and then washed twice with 1× PBS. A 2-ml aliquot of 2.4% Avicel overlay (FMC) was then added onto the infected cells, which were incubated for 3 days in an incubator at 37°C with 5% CO_2. After 3 days, Avicel overlays were removed and cells were washed with 1× PBS and fixed in 4% paraformaldehyde for 30 min at room temperature. Crystal violet (1%) was then added for 5 min to count plaques.

Statistical analysis. Statistical analysis was performed using Graph Pad Prism version 7. CFU data were log transformed to normalize distribution. Data are presented as mean values ± SEM. Significant differences ($P < 0.05$) were determined by Student's *t* test. Differences in fractions of mice that got sick were measured using Fisher's exact test. Survival analysis, including the kinetics by which mice succumb to infection, was performed using the log rank (Mantel-Cox) test. Asterisks indicate significant differences, and *P* values are noted in the figures.

SUPPLEMENTAL MATERIAL

Supplemental material is available online only.

SUPPLEMENTAL FILE 1, PDF file, 0.5 MB.

ACKNOWLEDGMENTS

We acknowledge James Nicholas Lee, Summer Schmaling, and Ognjen Sekulovic for technical assistance with clinical score, virus preparation, and nasal lavage, respectively. We also thank Andrew Camilli for bacterial strains and Marta Gaglia for protocols. They, along with Tim van Opijnen, Bharathi Sundaresh, and Marcia Osburne, provided important feedback on the manuscript.

Research reported in this publication was supported by the National Institutes of Health under award numbers R21 AG064215 to E.N.B.G., R01 HL151498 to B.A.D., and F31 AI122615-01A1 to S.E.R., and by the King Abdullah Scholarship Program (KASP) implemented by the Ministry of Higher Education (MOHE) under award number 7896504 to B.H.J.

REFERENCES

1. Kadioglu A, Weiser JN, Paton JC, Andrew PW. 2008. The role of *Streptococcus pneumoniae* virulence factors in host respiratory colonization and disease. Nat Rev Microbiol 6:288–301. https://doi.org/10.1038/nrmicro1871.
2. Chao Y, Marks LR, Pettigrew MM, Hakansson AP. 2014. *Streptococcus pneumoniae* biofilm formation and dispersion during colonization and disease. Front Cell Infect Microbiol 4:194. https://doi.org/10.3389/fcimb.2014.00194.
3. Marks LR, Parameswaran GI, Hakansson AP. 2012. Pneumococcal interactions with epithelial cells are crucial for optimal biofilm formation and colonization *in vitro* and *in vivo*. Infect Immun 80:2744–2760. https://doi.org/10.1128/IAI.00488-12.
4. Marks LR, Davidson BA, Knight PR, Hakansson AP. 2013. Interkingdom signaling induces *Streptococcus pneumoniae* biofilm dispersion and transition from asymptomatic colonization to disease. mBio 4:e00438-13. https://doi.org/10.1128/mBio.00438-13.
5. Blanchette-Cain K, Hinojosa CA, Akula Suresh Babu R, Lizcano A, Gonzalez-Juarbe N, Munoz-Almagro C, Sanchez CJ, Bergman MA, Orihuela CJ. 2013. *Streptococcus pneumoniae* biofilm formation is strain dependent, multifactorial, and associated with reduced invasiveness and immunoreactivity during colonization. mBio 4:e00745-13–e00713. https://doi.org/10.1128/mBio.00745-13.
6. Boe DM, Boule LA, Kovacs EJ. 2017. Innate immune responses in the ageing lung. Clin Exp Immunol 187:16–25. https://doi.org/10.1111/cei.12881.
7. Chong CP, Street PR. 2008. Pneumonia in the elderly: a review of the epidemiology, pathogenesis, microbiology, and clinical features. South Med J 101:1141–1145. quiz 1132, 1179. https://doi.org/10.1097/SMJ.0b013e318181d5b5.
8. Bogaert D, De Groot R, Hermans PW. 2004. *Streptococcus pneumoniae* colonisation: the key to pneumococcal disease. Lancet Infect Dis 4:144–154. https://doi.org/10.1016/S1473-3099(04)00938-7.
9. Simell B, Auranen K, Kayhty H, Goldblatt D, Dagan R, O'Brien KL, Pneumococcal Carriage G, Pneumococcal Carriage Group. 2012. The fundamental link between pneumococcal carriage and disease. Expert Rev Vaccines 11:841–855. https://doi.org/10.1586/erv.12.53.
10. Orsi A, Ansaldi F, Trucchi C, Rosselli R, Icardi G. 2016. Pneumococcus and the elderly in Italy: a summary of available evidence regarding carriage, clinical burden of lower respiratory tract infections and on-field effectiveness of PCV13 vaccination. Int J Mol Sci 17:1140. https://doi.org/10.3390/ijms17071140.
11. Smith EL, Wheeler I, Adler H, Ferreira DM, Sa-Leao R, Abdullahi O, Adetifa I, Becker-Dreps S, Esposito S, Farida H, Kandasamy R, Mackenzie GA, Nuorti JP, Nzenze S, Madhi SA, Ortega O, Roca A, Safari D, Schaumburg F, Usuf E, Sanders EAM, Grant LR, Hammitt LL, O'Brien KL, Gounder P, Bruden DJT, Stanton MC, Rylance J. 2020. Upper airways colonisation of Streptococcus pneumoniae in adults aged 60 years and older: a systematic review of prevalence and individual participant data meta-analysis of risk factors. J Infect 81:540–548. https://doi.org/10.1016/j.jinf.2020.06.028.
12. Regev-Yochay G, Raz M, Dagan R, Porat N, Shainberg B, Pinco E, Keller N, Rubinstein E. 2004. Nasopharyngeal carriage of *Streptococcus pneumoniae* by adults and children in community and family settings. Clin Infect Dis 38:632–639. https://doi.org/10.1086/381547.
13. Flamaing J, Peetermans WE, Vandeven J, Verhaegen J. 2010. Pneumococcal colonization in older persons in a nonoutbreak setting. J Am Geriatr Soc 58:396–398. https://doi.org/10.1111/j.1532-5415.2009.02700.x.
14. Palmu AA, Kaijalainen T, Saukkoriipi A, Leinonen M, Kilpi TM. 2012. Nasopharyngeal carriage of *Streptococcus pneumoniae* and pneumococcal urine antigen test in healthy elderly subjects. Scand J Infect Dis 44:433–438. https://doi.org/10.3109/00365548.2011.652162.
15. van Deursen AMM, van Houten MA, Webber C, Patton M, Scott D, Patterson S, Jiang Q, Gruber WC, Schmoele-Thoma B, Grobbee DE, Bonten MJM, Sanders EAM. 2018. The impact of the 13-valent pneumococcal conjugate vaccine on pneumococcal carriage in the Community Acquired Pneumonia Immunization Trial in Adults (CAPiTA) study. Clin Infect Dis 67:42–49. https://doi.org/10.1093/cid/ciy009.
16. Esposito S, Mari D, Bergamaschini L, Orenti A, Terranova L, Ruggiero L, Ierardi V, Gambino M, Croce FD, Principi N. 2016. Pneumococcal colonization in older adults. Immun Ageing 13:2. https://doi.org/10.1186/s12979-016-0057-0.

17. van Deursen AM, van den Bergh MR, Sanders EA, Carriage Pilot Study Group. 2016. Carriage of *Streptococcus pneumoniae* in asymptomatic, community-dwelling elderly in the Netherlands. Vaccine 34:4–6. https://doi.org/10.1016/j.vaccine.2015.11.014.
18. Krone CL, van de Groep K, Trzciński K, Sanders EAM, Bogaert D. 2014. Immunosenescence and pneumococcal disease: an imbalance in host-pathogen interactions. Lancet Respir Med 2:141–153. https://doi.org/10.1016/S2213-2600(13)70165-6.
19. Bou Ghanem EN, Clark S, Du X, Wu D, Camilli A, Leong JM, Meydani SN. 2015. The alpha-tocopherol form of vitamin E reverses age-associated susceptibility to *Streptococcus pneumoniae* lung infection by modulating pulmonary neutrophil recruitment. J Immunol 194:1090–1099. https://doi.org/10.4049/jimmunol.1402401.
20. Bou Ghanem EN, Clark S, Roggensack SE, McIver SR, Alcaide P, Haydon PG, Leong JM. 2015. Extracellular adenosine protects against *Streptococcus pneumoniae* lung infection by regulating pulmonary neutrophil recruitment. PLoS Pathog 11:e1005126. https://doi.org/10.1371/journal.ppat.1005126.
21. Garvy BA, Harmsen AG. 1996. The importance of neutrophils in resistance to pneumococcal pneumonia in adult and neonatal mice. Inflammation 20:499–512. https://doi.org/10.1007/BF01487042.
22. Hahn I, Klaus A, Janze AK, Steinwede K, Ding N, Bohling J, Brumshagen C, Serrano H, Gauthier F, Paton JC, Welte T, Maus UA. 2011. Cathepsin G and neutrophil elastase play critical and nonredundant roles in lung-protective immunity against *Streptococcus pneumoniae* in mice. Infect Immun 79:4893–4901. https://doi.org/10.1128/IAI.05593-11.
23. Simell B, Vuorela A, Ekstrom N, Palmu A, Reunanen A, Meri S, Kayhty H, Vakevainen M. 2011. Aging reduces the functionality of anti-pneumococcal antibodies and the killing of *Streptococcus pneumoniae* by neutrophil phagocytosis. Vaccine 29:1929–1934. https://doi.org/10.1016/j.vaccine.2010.12.121.
24. Bhalla MSS, Abamonte A, Herring SE, Roggensack SE, Bou Ghanem EN. 2020. Extracellular adenosine signaling reverses the age-driven decline in the ability of neutrophils to kill *S. pneumoniae*. Aging Cell 19:e13218. https://doi.org/10.1111/acel.13218.
25. Pignatti P, Ragnoli B, Radaeli A, Moscato G, Malerba M. 2011. Age-related increase of airway neutrophils in older healthy nonsmoking subjects. Rejuvenation Res 14:365–370. https://doi.org/10.1089/rej.2010.1150.
26. Menter T, Giefing-Kroell C, Grubeck-Loebenstein B, Tzankov A. 2014. Characterization of the inflammatory infiltrate in *Streptococcus pneumoniae* pneumonia in young and elderly patients. Pathobiology 81:160–167. https://doi.org/10.1159/000360165.
27. Bhowmick R, Maung N, Hurley BP, Ghanem EB, Gronert K, McCormick BA, Leong JM. 2013. Systemic disease during *Streptococcus pneumoniae* acute lung infection requires 12-lipoxygenase-dependent inflammation. J Immunol 191:5115–5123. https://doi.org/10.4049/jimmunol.1300522.
28. Bakaletz LO. 2017. Viral-bacterial co-infections in the respiratory tract. Curr Opin Microbiol 35:30–35. https://doi.org/10.1016/j.mib.2016.11.003.
29. McCullers JA. 2006. Insights into the interaction between influenza virus and pneumococcus. Clin Microbiol Rev 19:571–582. https://doi.org/10.1128/CMR.00058-05.
30. Chertow DS, Memoli MJ. 2013. Bacterial coinfection in influenza: a grand rounds review. JAMA 309:275–282. https://doi.org/10.1001/jama.2012.194139.
31. Centers for Disease Control and . 2010. Estimates of deaths associated with seasonal influenza—United States, 1976–2007. MMWR Morb Mortal Wkly Rep 59:1057–1062.
32. Shrestha S, Foxman B, Weinberger DM, Steiner C, Viboud C, Rohani P. 2013. Identifying the interaction between influenza and pneumococcal pneumonia using incidence data. Sci Transl Med 5:191ra84. https://doi.org/10.1126/scitranslmed.3005982.
33. McCullers JA. 2014. The co-pathogenesis of influenza viruses with bacteria in the lung. Nat Rev Microbiol 12:252–262. https://doi.org/10.1038/nrmicro3231.
34. Palacios G, Hornig M, Cisterna D, Savji N, Bussetti AV, Kapoor V, Hui J, Tokarz R, Briese T, Baumeister E, Lipkin WI. 2009. *Streptococcus pneumoniae* coinfection is correlated with the severity of H1N1 pandemic influenza. PLoS One 4:e8540. https://doi.org/10.1371/journal.pone.0008540.
35. Dhanoa A, Fang NC, Hassan SS, Kaniappan P, Rajasekaram G. 2011. Epidemiology and clinical characteristics of hospitalized patients with pandemic influenza A (H1N1) 2009 infections: the effects of bacterial coinfection. Virol J 8:501. https://doi.org/10.1186/1743-422X-8-501.
36. Siegel SJ, Roche AM, Weiser JN. 2014. Influenza promotes pneumococcal growth during coinfection by providing host sialylated substrates as a nutrient source. Cell Host Microbe 16:55–67. https://doi.org/10.1016/j.chom.2014.06.005.
37. Rowe HM, Meliopoulos VA, Iverson A, Bomme P, Schultz-Cherry S, Rosch JW. 2019. Direct interactions with influenza promote bacterial adherence during respiratory infections. Nat Microbiol 4:1328–1336. https://doi.org/10.1038/s41564-019-0447-0.
38. Diavatopoulos DA, Short KR, Price JT, Wilksch JJ, Brown LE, Briles DE, Strugnell RA, Wijburg OL. 2010. Influenza A virus facilitates *Streptococcus pneumoniae* transmission and disease. FASEB J 24:1789–1798. https://doi.org/10.1096/fj.09-146779.
39. Reddinger RM, Luke-Marshall NR, Sauberan SL, Hakansson AP, Campagnari AA. 2018. *Streptococcus pneumoniae* modulates *Staphylococcus aureus* biofilm dispersion and the transition from colonization to invasive disease. mBio 9:e02089-17. https://doi.org/10.1128/mBio.02089-17.
40. McCullers JA, Rehg JE. 2002. Lethal synergism between influenza virus and *Streptococcus pneumoniae*: characterization of a mouse model and the role of platelet-activating factor receptor. J Infect Dis 186:341–350. https://doi.org/10.1086/341462.
41. Levandowski RA, Gerrity TR, Garrard CS. 1985. Modifications of lung clearance mechanisms by acute influenza A infection. J Lab Clin Med 106:428–432.
42. Pittet LA, Hall-Stoodley L, Rutkowski MR, Harmsen AG. 2010. Influenza virus infection decreases tracheal mucociliary velocity and clearance of *Streptococcus pneumoniae*. Am J Respir Cell Mol Biol 42:450–460. https://doi.org/10.1165/rcmb.2007-0417OC.
43. McCullers JA, Bartmess KC. 2003. Role of neuraminidase in lethal synergism between influenza virus and *Streptococcus pneumoniae*. J Infect Dis 187:1000–1009. https://doi.org/10.1086/368163.
44. Smith AM, McCullers JA. 2014. Secondary bacterial infections in influenza virus infection pathogenesis. Curr Top Microbiol Immunol 385:327–356. https://doi.org/10.1007/82_2014_394.
45. Cundell DR, Gerard NP, Gerard C, Idanpaan-Heikkila I, Tuomanen EI. 1995. *Streptococcus pneumoniae* anchor to activated human cells by the receptor for platelet-activating factor. Nature 377:435–438. https://doi.org/10.1038/377435a0.
46. Ballinger MN, Standiford TJ. 2010. Postinfluenza bacterial pneumonia: host defenses gone awry. J Interferon Cytokine Res 30:643–652. https://doi.org/10.1089/jir.2010.0049.
47. Metzger DW, Sun K. 2013. Immune dysfunction and bacterial coinfections following influenza. J Immunol 191:2047–2052. https://doi.org/10.4049/jimmunol.1301152.
48. Sun K, Metzger DW. 2008. Inhibition of pulmonary antibacterial defense by interferon-gamma during recovery from influenza infection. Nat Med 14:558–564. https://doi.org/10.1038/nm1765.
49. Nakamura S, Davis KM, Weiser JN. 2011. Synergistic stimulation of type I interferons during influenza virus coinfection promotes *Streptococcus pneumoniae* colonization in mice. J Clin Invest 121:3657–3665. https://doi.org/10.1172/JCI57762.
50. Cho SJ, Plataki M, Mitzel D, Lowry G, Rooney K, Stout-Delgado H. 2018. Decreased NLRP3 inflammasome expression in aged lung may contribute to increased susceptibility to secondary *Streptococcus pneumoniae* infection. Exp Gerontol 105:40–46. https://doi.org/10.1016/j.exger.2017.11.010.
51. Krone CL, Wyllie AL, van Beek J, Rots NY, Oja AE, Chu MLJN, Bruin JP, Bogaert D, Sanders EAM, Trzciński K. 2015. Carriage of *Streptococcus pneumoniae* in aged adults with influenza-like-illness. PLoS One 10:e0119875. https://doi.org/10.1371/journal.pone.0119875.
52. Rello J, Pop-Vicas A. 2009. Clinical review: primary influenza viral pneumonia. Crit Care 13:235. https://doi.org/10.1186/cc8183.
53. Torres A, Loeches IM, Sligl W, Lee N. 2020. Severe flu management: a point of view. Intensive Care Med 46:153–162. https://doi.org/10.1007/s00134-019-05868-8.
54. Aaberge IS, Eng J, Lermark G, Lovik M. 1995. Virulence of *Streptococcus pneumoniae* in mice: a standardized method for preparation and frozen storage of the experimental bacterial inoculum. Microb Pathog 18:141–152. https://doi.org/10.1016/s0882-4010(95)90125-6.
55. Tettelin H, Nelson KE, Paulsen IT, Eisen JA, Read TD, Peterson S, Heidelberg J, DeBoy RT, Haft DH, Dodson RJ, Durkin AS, Gwinn M, Kolonay JF, Nelson WC, Peterson JD, Umayam LA, White O, Salzberg SL, Lewis MR, Radune D, Holtzapple E, Khouri H, Wolf AM, Utterback TR, Hansen CL, McDonald LA, Feldblyum TV, Angiuoli S, Dickinson T, Hickey EK, Holt IE, Loftus BJ, Yang F, Smith HO, Venter JC, Dougherty BA, Morrison DA, Hollingshead SK, Fraser CM. 2001. Complete genome sequence of a virulent isolate of *Streptococcus pneumoniae*. Science 293:498–506. https://doi.org/10.1126/science.1061217.

56. Bou Ghanem EN, Maung NHT, Siwapornchai N, Goodwin AE, Clark S, Munoz-Elias EJ, Camilli A, Gerstein RM, Leong JM. 2018. Nasopharyngeal exposure to *Streptococcus pneumoniae* induces extended age-dependent protection against pulmonary infection mediated by antibodies and CD138^{+} cells. J Immunol 200:3739–3751. https://doi.org/10.4049/jimmunol.1701065.
57. Bhalla M, Hui Yeoh J, Lamneck C, Herring SE, Tchalla EYI, Heinzinger LR, Leong JM, Bou Ghanem EN. 2020. A1 adenosine receptor signaling reduces *Streptococcus pneumoniae* adherence to pulmonary epithelial cells by targeting expression of platelet-activating factor receptor. Cell Microbiol 22:e13141. https://doi.org/10.1111/cmi.13141.
58. Boyd AR, Shivshankar P, Jiang S, Berton MT, Orihuela CJ. 2012. Age-related defects in TLR2 signaling diminish the cytokine response by alveolar macrophages during murine pneumococcal pneumonia. Exp Gerontol 47:507–518. https://doi.org/10.1016/j.exger.2012.04.004.
59. Thevaranjan N, Puchta A, Schulz C, Naidoo A, Szamosi JC, Verschoor CP, Loukov D, Schenck LP, Jury J, Foley KP, Schertzer JD, Larche MJ, Davidson DJ, Verdu EF, Surette MG, Bowdish DME. 2018. Age-associated microbial dysbiosis promotes intestinal permeability, systemic inflammation, and macrophage dysfunction. Cell Host Microbe 23:570. https://doi.org/10.1016/j.chom.2018.03.006.
60. McNamee LA, Harmsen AG. 2006. Both influenza-induced neutrophil dysfunction and neutrophil-independent mechanisms contribute to increased susceptibility to a secondary *Streptococcus pneumoniae* infection. Infect Immun 74:6707–6721. https://doi.org/10.1128/IAI.00789-06.
61. Bou Ghanem EN, Lee JN, Joma BH, Meydani SN, Leong JM, Panda A. 2017. The alpha-tocopherol form of vitamin E boosts elastase activity of human PMNs and their ability to kill *Streptococcus pneumoniae*. Front Cell Infect Microbiol 7:161. https://doi.org/10.3389/fcimb.2017.00161.
62. Wu W, Metcalf JP. 2020. The role of type I IFNs in influenza: antiviral superheroes or immunopathogenic villains? J Innate Immun 12:437–447. https://doi.org/10.1159/000508379.
63. Wagenvoort GH, Sanders EA, Vlaminckx BJ, de Melker HE, van der Ende A, Knol MJ. 2017. Sex differences in invasive pneumococcal disease and the impact of pneumococcal conjugate vaccination in the Netherlands, 2004 to 2015. Euro Surveill 22(10):pii=30481. https://www.eurosurveillance.org/content/10.2807/1560-7917.ES.2017.22.10.30481.
64. Gutierrez F, Masia M, Mirete C, Soldan B, Rodriguez JC, Padilla S, Hernandez I, Royo G, Martin-Hidalgo A. 2006. The influence of age and gender on the population-based incidence of community-acquired pneumonia caused by different microbial pathogens. J Infect 53:166–174. https://doi.org/10.1016/j.jinf.2005.11.006.
65. Greene CJ, Marks LR, Hu JC, Reddinger R, Mandell L, Roche-Hakansson H, King-Lyons ND, Connell TD, Hakansson AP. 2016. Novel strategy to protect against influenza virus-induced pneumococcal disease without interfering with commensal colonization. Infect Immun 84:1693–1703. https://doi.org/10.1128/IAI.01478-15.
66. Mina MJ, Klugman KP, McCullers JA. 2013. Live attenuated influenza vaccine, but not pneumococcal conjugate vaccine, protects against increased density and duration of pneumococcal carriage after influenza infection in pneumococcal colonized mice. J Infect Dis 208:1281–1285. https://doi.org/10.1093/infdis/jit317.
67. Wadowsky RM, Mietzner SM, Skoner DP, Doyle WJ, Fireman P. 1995. Effect of experimental influenza A virus infection on isolation of *Streptococcus pneumoniae* and other aerobic bacteria from the oropharynges of allergic and nonallergic adult subjects. Infect Immun 63:1153–1157. https://doi.org/10.1128/IAI.63.4.1153-1157.1995.
68. Jochems SP, Marcon F, Carniel BF, Holloway M, Mitsi E, Smith E, Gritzfeld JF, Solorzano C, Reine J, Pojar S, Nikolaou E, German EL, Hyder-Wright A, Hill H, Hales C, de Steenhuijsen Piters WAA, Bogaert D, Adler H, Zaidi S, Connor V, Gordon SB, Rylance J, Nakaya HI, Ferreira DM. 2018. Inflammation induced by influenza virus impairs human innate immune control of pneumococcus. Nat Immunol 19:1299–1308. https://doi.org/10.1038/s41590-018-0231-y.
69. Stout-Delgado HW, Vaughan SE, Shirali AC, Jaramillo RJ, Harrod KS. 2012. Impaired NLRP3 inflammasome function in elderly mice during influenza infection is rescued by treatment with nigericin. J Immunol 188:2815–2824. https://doi.org/10.4049/jimmunol.1103051.
70. Gay R, Han SN, Marko M, Belisle S, Bronson R, Meydani SN. 2004. The effect of vitamin E on secondary bacterial infection after influenza infection in young and old mice. Ann N Y Acad Sci 1031:418–421. https://doi.org/10.1196/annals.1331.061.
71. Smith MW, Schmidt JE, Rehg JE, Orihuela CJ, McCullers JA. 2007. Induction of pro- and anti-inflammatory molecules in a mouse model of pneumococcal pneumonia after influenza. Comp Med 57:82–89.
72. McNeela EA, Burke A, Neill DR, Baxter C, Fernandes VE, Ferreira D, Smeaton S, El-Rachkidy R, McLoughlin RM, Mori A, Moran B, Fitzgerald KA, Tschopp J, Petrilli V, Andrew PW, Kadioglu A, Lavelle EC. 2010. Pneumolysin activates the NLRP3 inflammasome and promotes proinflammatory cytokines independently of TLR4. PLoS Pathog 6:e1001191. https://doi.org/10.1371/journal.ppat.1001191.
73. Pettigrew MM, Marks LR, Kong Y, Gent JF, Roche-Hakansson H, Hakansson AP. 2014. Dynamic changes in the *Streptococcus pneumoniae* transcriptome during transition from biofilm formation to invasive disease upon influenza A virus infection. Infect Immun 82:4607–4619. https://doi.org/10.1128/IAI.02225-14.
74. Siwapornchai N, Lee JN, Tchalla EYI, Bhalla M, Yeoh JH, Roggensack SE, Leong JM, Bou Ghanem EN. 2020. Extracellular adenosine enhances the ability of PMNs to kill *Streptococcus pneumoniae* by inhibiting IL-10 production. J Leukoc Biol 108:867–882. https://doi.org/10.1002/JLB.4MA0120-115RR.
75. Short KR, Reading PC, Wang N, Diavatopoulos DA, Wijburg OL. 2012. Increased nasopharyngeal bacterial titers and local inflammation facilitate transmission of *Streptococcus pneumoniae*. mBio 3:e00255-12. https://doi.org/10.1128/mBio.00255-12.
76. Kulkarni U, Zemans RL, Smith CA, Wood SC, Deng JC, Goldstein DR. 2019. Excessive neutrophil levels in the lung underlie the age-associated increase in influenza mortality. Mucosal Immunol 12:545–554. https://doi.org/10.1038/s41385-018-0115-3.
77. van der Sluijs KF, van Elden LJ, Nijhuis M, Schuurman R, Pater JM, Florquin S, Goldman M, Jansen HM, Lutter R, van der Poll T. 2004. IL-10 is an important mediator of the enhanced susceptibility to pneumococcal pneumonia after influenza infection. J Immunol 172:7603–7609. https://doi.org/10.4049/jimmunol.172.12.7603.
78. Feng E, Balint E, Poznanski SM, Ashkar AA, Loeb M. 2021. Aging and interferons: impacts on inflammation and viral disease outcomes. Cells 10:708. https://doi.org/10.3390/cells10030708.
79. Rowe HM, Livingston B, Margolis E, Davis A, Meliopoulos VA, Echlin H, Schultz-Cherry S, Rosch JW. 2020. Respiratory bacteria stabilize and promote airborne transmission of influenza A virus. mSystems 5:e00762-20. https://doi.org/10.1128/mSystems.00762-20.
80. Nguyen DT, Louwen R, Elberse K, van Amerongen G, Yuksel S, Luijendijk A, Osterhaus AD, Duprex WP, de Swart RL. 2015. *Streptococcus pneumoniae* enhances human respiratory syncytial virus infection *in vitro* and *in vivo*. PLoS One 10:e0127098. https://doi.org/10.1371/journal.pone.0127098.
81. Carniel BF, Marcon F, Rylance J, German EL, Zaidi S, Reine J, Negera E, Nikolaou E, Pojar S, Solorzano C, Collins AM, Connor V, Bogaert D, Gordon SB, Nakaya HI, Ferreira DM, Jochems SP, Mitsi E. 2021. Pneumococcal colonization impairs mucosal immune responses to live attenuated influenza vaccine. JCI Insight 6:e141088. https://doi.org/10.1172/jci.insight.141088.
82. Swamydas M, Lionakis MS. 2013. Isolation, purification and labeling of mouse bone marrow neutrophils for functional studies and adoptive transfer experiments. J Vis Exp (77):e50586. https://doi.org/10.3791/50586.
83. Nishina K, Mikawa K, Takao Y, Shiga M, Maekawa N, Obara H. 1998. Intravenous lidocaine attenuates acute lung injury induced by hydrochloric acid aspiration in rabbits. Anesthesiology 88:1300–1309. https://doi.org/10.1097/00000542-199805000-00022.